SUPPLEMENTARY FIGURES

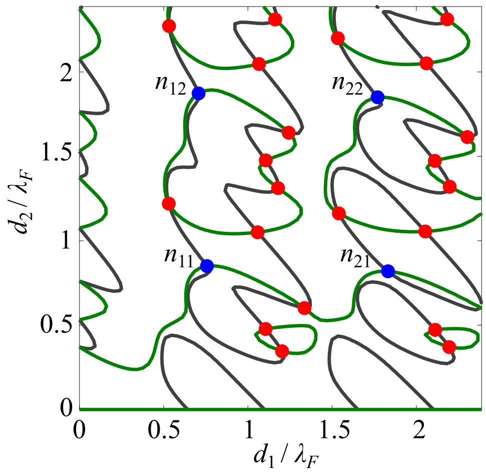

Figure 1. The symmetric bouncing states for a chain of $N = 5$ drops are computed using the procedure described in §3.2 of the Main Text. The gray and green curves in the figure denote the zero-contours of the the functions $F_1(d_1, d_2)$ and $F_2(d_1, d_2)$, respectively, defined in Eq. (8) in the Main Text. Here, d_1 is the distance between the first and second drop, which equals that between the fourth and fifth drop; d_2 is the distance between the second and third drop, which equals that between the third and fourth drop. The intersections of the contours correspond to bouncing states, which are color-coded on the basis of the linear stability analysis presented in §3.1 of the Main Text. Specifically, blue (red) dots denote stable (unstable) solutions at the lowest memory considered, $\gamma/\gamma_F = 0.66$. The stable states are labeled n_{11}, n_{12}, n_{21} and n_{22}. The Faraday wavelength is denoted by λ_F.

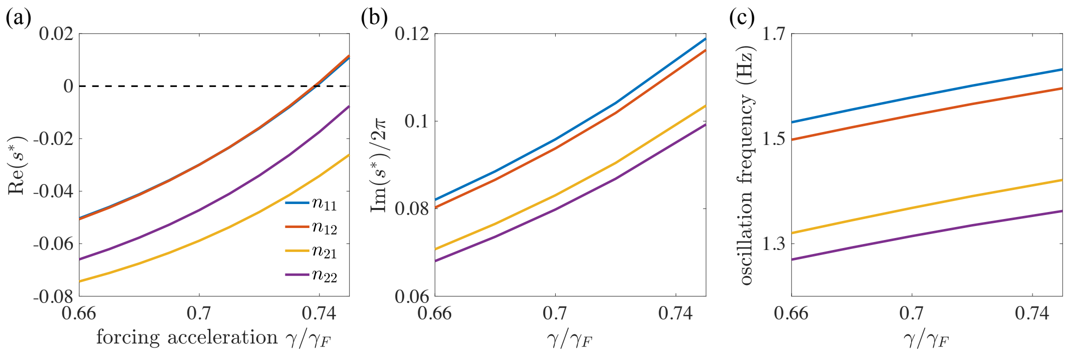

Figure 2. Stability analysis of symmetric bouncing states of a five-droplet chain, performed using the procedure described in §3.1 of the Main Text. Specifically, s^* denotes the nontrivial eigenvalue of the matrix Q with the largest real part, where Q is defined in Eq. (7) in the Main Text. Colors denote the different bouncing states n_{11}, n_{12}, n_{21} and n_{22}, as shown in the legend of panel (a). The dimensionless forcing acceleration of the bath is denoted γ/γ_F. (a) Real part of s^*, which determines the stability of the bouncing state, $\text{Re}(s^*) < 0$ ($\text{Re}(s^*) > 0$) corresponding to stable (unstable) states. (b) Imaginary part of s^*. (c) The dimensional oscillation frequency $\text{Im}(s^*)/(2\pi T_M)$ of the chain, T_M being the memory time defined in Eq. (2) in the Main Text.

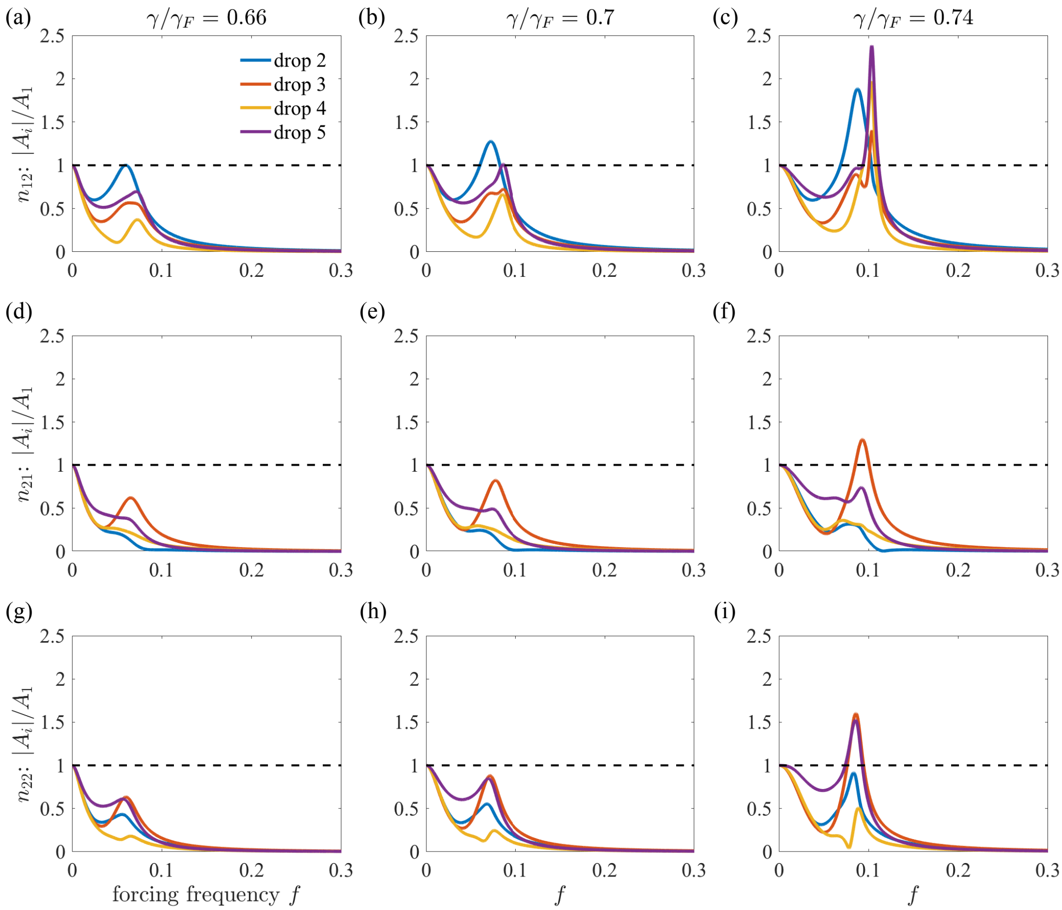

Figure 3. The figures show the dependence of the oscillation amplitude $|A_i|$ on the dimensionless forcing frequency f for a periodically-forced chain of five drops, as computed using the linear theory presented in §4.1 of the Main Text. The procedure described in the caption of Fig. 3 in the Main Text is repeated for droplet chains initialized in the n_{12} (panels (a)–(c)), n_{21} (panels (d)–(f)), and n_{22} (panels (g)–(i)) bouncing states. Three values of the bath's forcing acceleration are shown: $\gamma/\gamma_F = 0.66$ (left panels), $\gamma/\gamma_F = 0.7$ (middle panels) and $\gamma/\gamma_F = 0.74$ (right panels).

https://doi.org/10.5802/crmeca.30

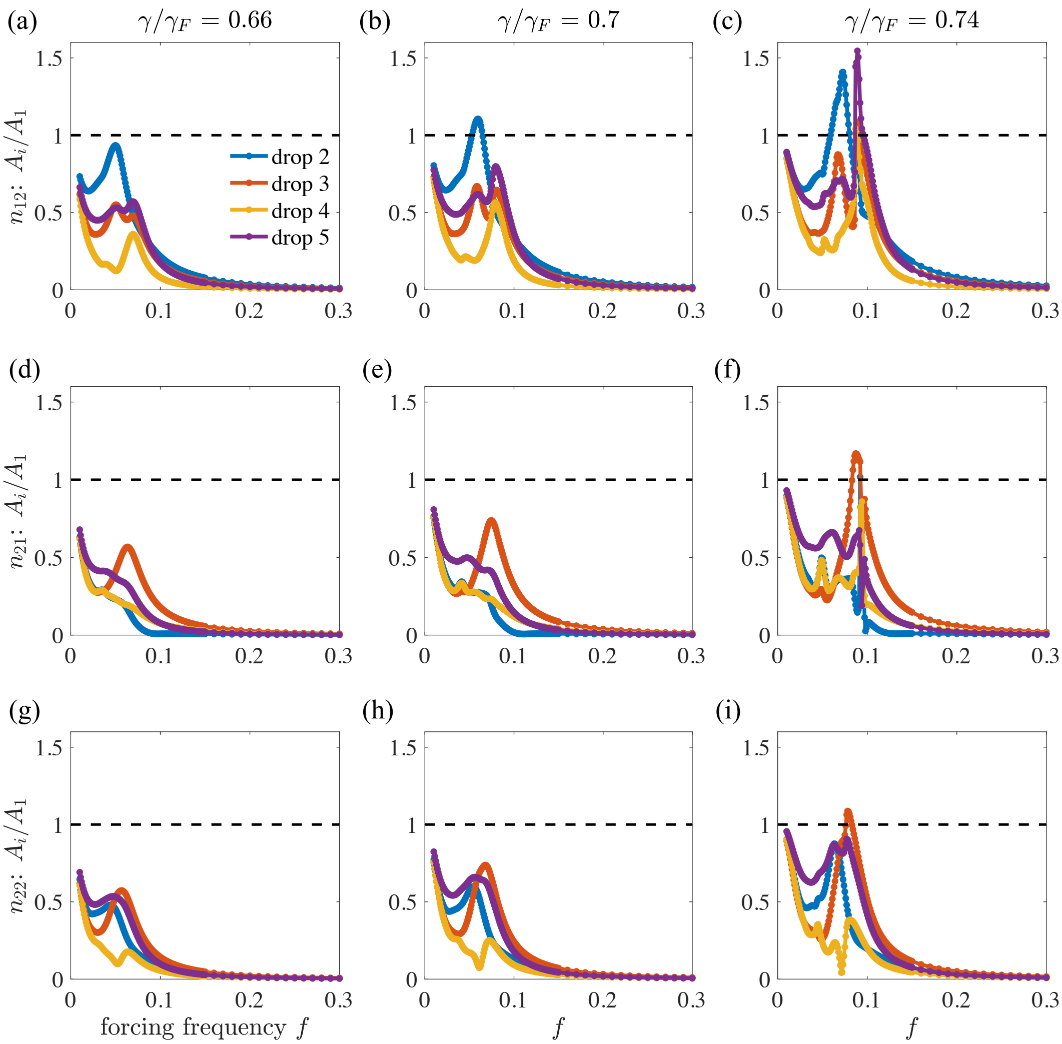

Figure 4. The figures show the dependence of the oscillation amplitude A_i on the dimensionless forcing frequency f for a periodically-forced chain of five drops. The amplitudes are computed using numerical simulations of the trajectory equation (3) in the Main Text. Specifically, the procedure described in the caption of Fig. 5 in the Main Text is repeated for droplet chains initialized in the n_{12} (panels (a)–(c)), n_{21} (panels (d)–(f)), and n_{22} (panels (g)–(i)) bouncing states. Three values of the bath's forcing acceleration are shown: $\gamma/\gamma_F = 0.66$ (left panels), $\gamma/\gamma_F = 0.7$ (middle panels) and $\gamma/\gamma_F = 0.74$ (right panels).

https://doi.org/10.5802/crmeca.30

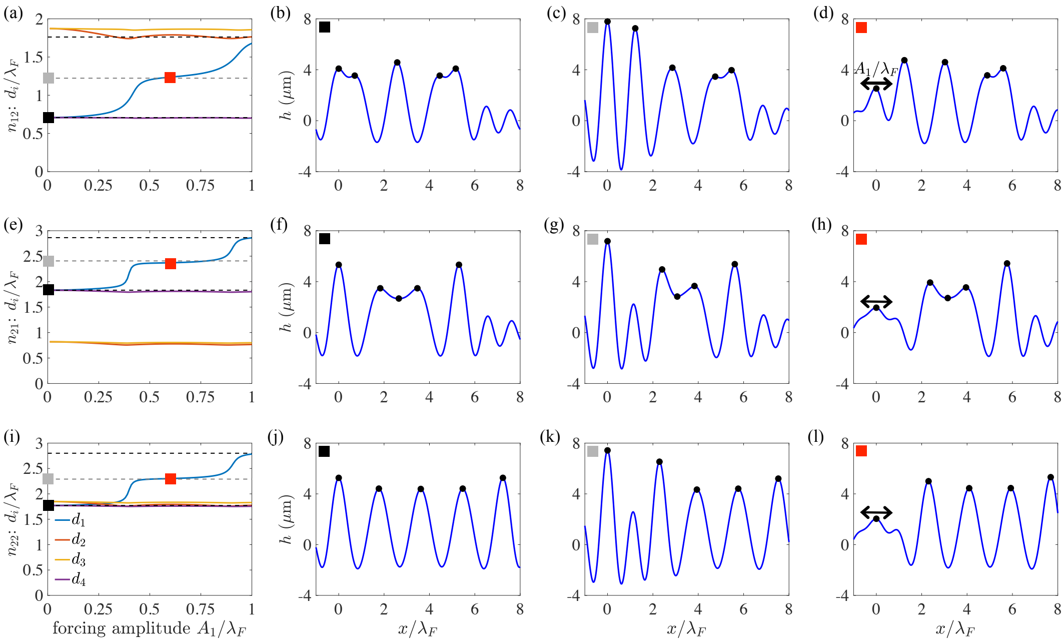

Figure 5. Bouncing states of a chain of five drops obtained in the limit of high forcing frequency, $f \to \infty$. The procedure in Fig. 8 of the Main Text is repeated for chains initialized in the bouncing states n_{12} (panels (a)–(d)), n_{21} (panels (e)–(h)), and n_{22} (panels (i)–(l)).

https://doi.org/10.5802/crmeca.30